THE JOURNAL OF PHYSICAL CHEMISTRY B

Article

pubs.acs.org/JPCB

Inclusion of Chloromethane Guests Affects Conformation and Internal Dynamics of Cryptophane-D Host

Zoltan Takacs,*[,†] Thierry Brotin,[‡] Jean-Pierre Dutasta,[‡] Jan Lang,[§] Guido Todde,[†] and Jozef Kowalewski*[,†]

[†]Department of Materials and Environmental Chemistry, Arrhenius Laboratory, Stockholm University, S-10691 Stockholm, Sweden

[‡]Laboratoire de Chimie (CNRS-UMR, 5182), Ecole Normale Superieure de Lyon, 46 Allèe d'Italie, 69364 Lyon cedex 07, France

[§]Department of Low Temperature Physics, Faculty of Mathematics and Physics, Charles University in Prague, V Holesovickach 2, CZ-180 00 Prague 8, Czech Republic

Supporting Information

ABSTRACT: Cryptophane-D is composed of two nonequivalent cyclotribenzylene caps bound together by three OCH_2CH_2O bridges in a syn arrangement. Host−guest complexes with chloroform and dichloromethane were investigated in solution by NMR spectroscopy. Variable temperature NMR ^1H and ^{13}C spectra showed effects of chemical exchange between the free and bound guest and of conformational exchange for the host, strongly and specifically affected by guest binding. We found in particular that the carbon-13 chemical shifts for the linkers connecting the two cyclotribenzylene units are very informative. The NMR results were supported by DFT calculations. The guest exchange was also studied quantitatively, either by EXSY measurements (for chloroform as guest) or by line-shape analysis (for dichloromethane as guest). In the case of chloroform guest, we also investigated cross-relaxation between the guest and host protons, as well as carbon-13 longitudinal relaxation and heteronuclear NOE at three different fields. The results were interpreted in terms of orientation and dynamics of the guest inside the host cavity. Putting together various types of evidence resulted in remarkably detailed insight into the process of molecular recognition of the two guests by cryptophane-D host.

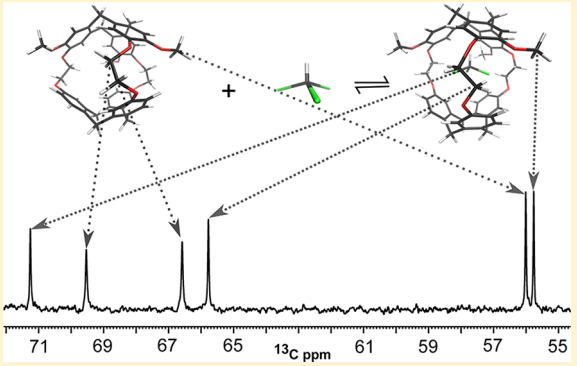

INTRODUCTION

Cryptophanes are able to encapsulate small organic molecules which makes these compounds interesting for investigation of intermolecular van der Waals interactions. Cryptophanes are composed of two cyclotribenzylene (CTB) caps which are bound together by aliphatic linkers providing a hydrophobic three-dimensional cavity.[1] The size of the cavity depends on the length of the linkers. Different groups can be attached to the CTB rings, in the case of of cryptophane-A[2] there is a methoxy group on each phenyl ring of the two CTBs. This makes the two caps equivalent, giving the molecule a maximum D_3 symmetry. Cryptophane-C and -D[2] have methoxy groups attached only to one of the CTB rings. Thus, the symmetry is reduced to maximum C_3. All three cryptophanes mentioned above (A, C, D) have ethylenedioxy linkers and the maximum symmetry is fulfilled only if the three linkers have the same conformation, i.e. they have the same OCCO dihedral angles. We are going to denote such conformations all-gauche or *GGG* and all-trans (*TTT*). In all other cases (*GGT*,*GTT*) the molecule belongs to *C*1 symmetry group. Actually, there are two types of trans and four types of gauche conformation (see below). Cryptophane-D is the syn isomer of cryptophane-C.[1] The size of the cavity is somewhat bigger in the case of the syn isomer. The molecule is also axially chiral. The solutions investigated in this work are racemic mixtures of enantiomers (Scheme 1). NMR is blind to chirality and hence there is no difference seen between the enantiomers in the spectra.

Very recently, Taratula et al. proposed utilization of cryptophane-A and two of its water-soluble derivatives as model systems for exploration of molecular recognition in the case of noncovalent complexes held by London forces.[3] They documented very convincingly by means of X-ray crystallography that the volume of cryptophane cavity varied by more than 20% in the series of guests water, methanol, xenon, and chloroform (ordered by increasing molecular volume). Understanding that the changes in conformation of ethylenedioxy linkers are the major mechanism of the cavity adaptation is well established now.[4−8] Nevertheless, molecular recognition is an inherently dynamical phenomenon, and it cannot be fully explained on the basis of experimental methods providing a largely static view of molecular structures. We wish to contribute to the ongoing debate by detailed measurements

Received: April 11, 2012
Revised: June 8, 2012
Published: June 12, 2012

dx.doi.org/10.1021/jp303469x | *J. Phys. Chem. B* 2012, 116, 7898−7913

Scheme 1. All trans Conformer of Crytophane-D with Atom Numbering and Its Enantiomer Mirror Image

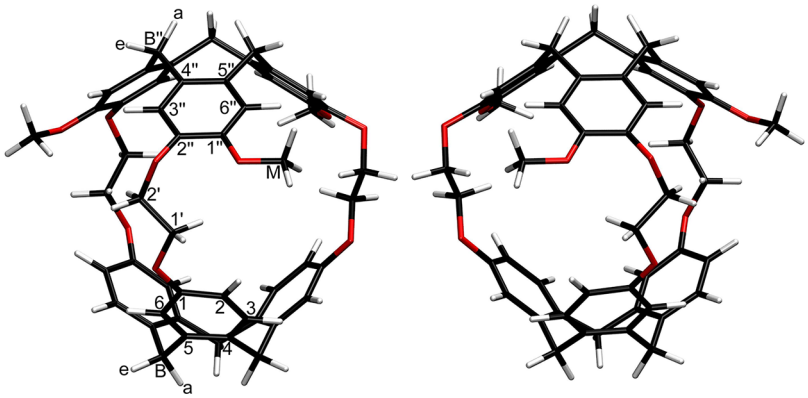

of dynamic aspects of formation of cryptophane-D inclusion complexes with two neutral guests of different size: dichloromethane and chloroform.

Encapsulation of a guest molecule into the cavity can be investigated by NMR spectroscopy since the bound guest has a big chemical shift difference compared to the free guest. We follow here the ^{1}H and ^{13}C spectra as a function of sample composition and temperature. The complexed guest nuclei are more shielded compared to the free guest. This allows us to get information about the rate of guest exchange between the free and bound sites. This is usually done by means of exchange spectroscopy (EXSY) on protons or through line-shape analysis. These processes occur on the NMR chemical shift time scale, together with the conformational changes of the linkers. In analogy with our previous work on $CHCl_3$@cryptophane-C,[9] we also explore the dipole−dipole interactions of chloroform inside the cavity with phenyl protons in the nonequivalent caps using 1D ^{1}H NOESY and ROESY cross-relaxation experiments. Moreover, we also study the mobility of the guest inside the cavity by measuring the relaxation parameters (T_1 and heteronuclear NOE) of the carbon-13 nucleus.[10−12]

As a complement to the NMR work, we have also performed quantum chemical calculations on the level of density functional theory (DFT). Such calculations have a dual purpose. First, they can provide information about the energetics and thus the Boltzmann distribution of conformers of the cryptophane in the free state as well as in complex. In addition, one can calculate the changes in ^{13}C chemical shifts upon conformational changes and complex formation. The calculations can be helpful in rationalizing the changes observed in the experimental spectra.

The outline of this paper is as follows. We begin by recapitulating briefly the main features of the NMR methods used, followed by the description of experimental details. Next, we present and discuss the results for cryptophane-D samples without added chloroform and proceed to the data in the cryptophane-D−dichloromethane and cryptophane-D−chloroform systems containing excess of guests over the host.

METHODS

Kinetics of Complex Formation. The complexation reaction between the host (H) and the guest (G) can be approximated as a pseudofirst-order and the decomplexation reaction is a first-order reaction as is described by eqs 1 and 2

$$\mathrm{H} + \mathrm{G} \underset{k_{-1}}{\overset{k_1}{\rightleftharpoons}} \mathrm{HG} \tag{1}$$

$$\frac{-\mathrm{d}[\mathrm{G}]}{\mathrm{d}t} = k_1[\mathrm{H}][\mathrm{G}] = k'_1[\mathrm{G}] \text{ and } \frac{-\mathrm{d}[\mathrm{HG}]}{\mathrm{d}t} = k_{-1}[\mathrm{HG}] \tag{2}$$

$$k'_1 = k_1[H] = k_{\mathrm{fb}} \text{ and } k_{-1} = k_{\mathrm{bf}} \tag{3}$$

$$K = \frac{k_1}{k_{-1}} = \frac{k_{\mathrm{fb}}}{[\mathrm{H}]k_{\mathrm{bf}}} = \frac{[\mathrm{HG}]}{[\mathrm{H}][\mathrm{G}]} \tag{4}$$

$$k_{\mathrm{fb}}M_{[\mathrm{G}]} = k_{\mathrm{bf}}M_{[\mathrm{HG}]} \Rightarrow k_{\mathrm{fb}} = \frac{k_{\mathrm{bf}}M_{[\mathrm{HG}]}}{M_{[\mathrm{G}]}} \tag{5}$$

where [H] and [G] denote the concentration of the free host and the free guest, respectively. The concentration of bound guest and bound host is the same and is denoted by [HG]. The symbols k_{fb} and k_{bf} correspond to the experimentally observed build-up rates for NMR signal at one of the sites after a selective excitation of the spins in the other site in the exchange spectroscopy (EXSY) experiment (assuming that the exchange process is slow enough). The reaction rate constant k_1 can be determined from the measured rate constant and the concentration of the free host. K is the equilibrium constant for complex formation. Again, if the exchange is slow enough, then the equilibrium constant can be determined either from the ratio of concentrations, obtained through integration of the proton signals, or from the ratio of the rates. Our experience is that the two methods give results in good agreement with each other.[10,11] Equation 5 is just the principle of detailed balance ($M_{[\mathrm{G}]}$ and $M_{[\mathrm{HG}]}$ are the z magnetizations of the free and bound guest). In fact, we make use of eq 5 to determine the value of k_{fb} from the integrals taken from a ^{1}H spectrum and from k_{bf}. In the "initial rate regime", at short build-up time intervals (τ_{mix}), the build-up curve is linear and makes it possible to extract the reaction rates. These measurements are usually carried out both for the free and bound site giving directly the two reaction rates. In our case, however, the bound signal intensity in the experiments that measure the rate k_{fb} is very low at small mixing times and hence carries a big error. In order to avoid these big measurement uncertainties, we just performed the measurement of k_{bf} and then used the principle of detailed balance to get k_{fb}.

If the exchange is so fast that it causes substantial line-broadening and distortions of the line positions (the medium fast and fast exchange regimes), then both the rate constants

dx.doi.org/10.1021/jp303469x | J. Phys. Chem. B 2012, 116, 7898−7913

and the equilibrium constants can be determined by line-shape analysis of either proton or carbon-13 spectra. The method is based on line-shape theories.[13,14] The simplest case, two-site exchange of the guest molecule where there are no scalar couplings involved, can be modeled with the modified Bloch–McConnell equations.[15] In any other case, when scalar couplings are present, the density matrix approach holds as it was described by Binsch[13] and Bain and Duns.[16]

Relaxation. The relaxation properties of ^{13}C nucleus carry information about the dynamics of the free host, free guest, and bound guest. The measurement of the spin–lattice relaxation rate is performed with broadband irradiation of the protons, and by doing so, the relaxation of the ^{13}C in the absence of exchange is single exponential.[17] The dominant relaxation mechanism for the proton-carrying carbons is the dipole–dipole (DD) interaction with protons. For aromatic carbons, where the chemical shift anisotropy (CSA) is large, the CSA mechanism should also be taken into account. The nuclear Overhauser enhancement (NOE) also carries valuable information about the dynamics of the molecular site in question. These factors are expressed in terms of spectral densities at the linear combination of ^1H and ^{13}C frequencies in eq 6 and 7,[10,17] where ω_C and ω_H are the Larmor frequencies of ^{13}C and ^1H, γ_C and γ_H are the magnetogyric ratios of ^{13}C and ^1H, respectively, and $\hbar$ is the Planck constant divided by 2π. The dipolar coupling constant (DCC) is denoted b_{CH} and N_H is the number of protons bound to the ^{13}C nucleus in question. The spin–lattice relaxation of aromatic carbons is driven by both the DD interaction and the CSA. The factor $\Delta\sigma$ in eq 7 is the magnitude of the CSA. As it can be seen from eq 7, the CSA relaxation rate scales as the magnetic field squared so it contributes to the relaxation more at higher magnetic field.

$$T_{1DD}^{-1} = \frac{1}{4}N_H {b_{CH}}^2[J(\omega_H - \omega_C) + 3J(\omega_C) + 6J(\omega_H + \omega_C)] \quad (6)$$

$$T_{1CSA}^{-1} = \frac{1}{3}(\gamma_C B_0 \Delta\sigma)^2 J(\omega_C) \quad (7)$$

$$T_{1obs}^{-1} = T_{1DD}^{-1} + T_{1CSA}^{-1} \quad (8)$$

$$\mathrm{NOE} = 1 + \eta \quad (9)$$

$$\eta = \frac{1}{4}\left(\frac{\gamma_H}{\gamma_C}\right) T_1 N_H {b_{CH}}^2[6J(\omega_H + \omega_C) - J(\omega_H - \omega_C)] \quad (10)$$

$$b_{CH} = -\frac{\mu_0 \gamma_H \gamma_C \hbar}{4\pi {r_{CH}}^3} \quad (11)$$

The combination of spectral densities in the numerator in eq 10 is proportional to the cross-relaxation rate (σ_{CH}).

If the ^{13}C site in question is in exchange with a rate similar to the relaxation rates, then the above statement of the longitudinal relaxation being single exponential does not hold any more. The relaxation becomes multiexponential according to the number of sites in exchange. In our case this means the relaxation of the ^{13}C nuclei in the guest becomes double-exponential because we have only two sites in exchange. All of the relaxation rates were measured with proton broadband decoupling, and hence, we have a single ^{13}C peak for each site. This allows us to use the modified Bloch equations for the magnetizations of the two sites.[15,18−21] If the relaxation rates are measured with the inversion–recovery methods, then they can be expressed as in eq 12

$$\frac{d}{dt}\begin{pmatrix} I_F \\ I_B \end{pmatrix} = \begin{pmatrix} -R_F - k_{fb} & k_{bf} \\ k_{fb} & -R_B - k_{bf} \end{pmatrix}\begin{pmatrix} I_F \\ I_B \end{pmatrix} + \begin{pmatrix} R_F & 0 \\ 0 & R_B \end{pmatrix}\begin{pmatrix} {I^*}_F \\ {I^*}_B \end{pmatrix} \quad (12)$$

In eq 12 R_F and R_B are the relaxation rates for the free and bound sites, respectively, k_{fb} and k_{bf} are the buildup-rates. I_F* and I_B* are NOE-enhanced intensities in the absence of exchange. The expression for the NOE enhancement can be derived from the full Bloch–McConnell and from the principle of detailed balance and is shown in eqs 13 and 14.

$$\mathrm{NOE}_F = \frac{R_F + k_{fb}}{R_F}\mathrm{NOE}_F^{obs} - \frac{k_{fb}}{R_F}\mathrm{NOE}_B^{obs} \quad (13)$$

$$\mathrm{NOE}_B = \frac{R_B + k_{bf}}{R_B}\mathrm{NOE}_B^{obs} - \frac{k_{bf}}{R_B}\mathrm{NOE}_F^{obs} \quad (14)$$

NOE_f^{obs} and NOE_B^{obs} are the measured enhancements.

The form of the spectral density function, in eqs 6, 7, and 10, depends on the motional model chosen for description of the reorientational dynamics of the molecule. We use in this work the Lipari-Szabo ("model-free") approach both for the host and for the bound guest. This model assumes isotropic overall reorientation of the whole molecule and, uncorrelated to this, a faster anisotropic local reorientation.[12,22] The former is characterized by a correlation time (τ_G) and the latter by a correlation time (τ_{loc}) and a generalized order parameter (S^2), which gives information about the spatial restrictions of the internal motion (eq 15). If the order parameter is high (larger than about 0.8), one can neglect the second term of eq 15 since it becomes very small. By doing this, we arrive at the truncated Lipari–Szabo approach (eq 16) that is very similar to the spectral density describing isotropic reorientation.

$$J(\omega) = \frac{2}{5}\left[\frac{S^2\tau_G}{1 + \omega^2{\tau_G}^2} + \frac{(1 - S^2)\tau}{1 + \omega^2\tau^2}\right] \quad (15)$$

$$J(\omega) = \frac{2}{5}\left[\frac{S^2\tau_G}{1 + \omega^2{\tau_G}^2}\right] \quad (16)$$

$$\tau^{-1} = \tau_G^{-1} + \tau_{loc}^{-1} \quad (17)$$

In the analysis of the ^{13}C relaxation for the host–guest complex, we make a simplifying assumption that the global reorientation of the host is only weakly modified by the encapsulation of the guest.

^1H-^1H Cross-Relaxation. The relaxation processes in spin systems with dipolar interactions are in general multi-exponential, as shown in the case of two spins by Solomon already in 1955.[23] This feature is caused by cross-relaxation between pairs of spins. The cross-relaxation rate depends on the inverse sixth power of the distance between spins. Homonuclear cross-relaxation measurements can be done as one- or two-dimensional experiments, and in the laboratory frame (NOESY) or in the rotating frame (ROESY). The two methods carry essentially the same information. They are used to map dipolarly coupled spin pairs, which can provide

dx.doi.org/10.1021/jp303469x | J. Phys. Chem. B 2012, 116, 7898–7913

structural information. The one-dimensional (1D) measurement requires a selective excitation of a certain bandwidth. Depending on the required bandwidth, an appropriate shaped pulse is used to excite the region. The 1D NOESY experiment is identical to the 1D EXSY experiment measuring the chemical exchange. The two-dimensional (2D) experiment is favored if there are many spin sites of interest. In this work, the 2D measurements are used to get qualitative information about the connectivities while the quantitative data for measuring the exchange rates and cross-relaxation rates are obtained in 1D measurements. The investigation of cross-relaxation between protons in the guest and in the host can provide information about the possible orientation of the guest through mapping the dipole−dipole interactions inside the cavity. If the reorientational motion of the host is sufficiently slow, then the 2D cross-peaks coming from exchange and cross-relaxation have the same phase in the conventional laboratory frame experiment. In the rotating frame cross-relaxation experiments the exchange and cross-relaxation rates have opposite phase. The intensities of cross-peaks decay also with distance as r_{AB}^{-6} and there are no cross-peak expected from spins being more than 6 Å away from each other.

Method of Error Estimation. The data analysis accumulates the error[12] from the measurement to the parameters. The error estimation is based on the Monte Carlo method. The data analysis has been repeated 1000 times with estimated measurement error included and the deviation of the model from measurement was determined. The error is expressed in the form of standard deviation.

EXPERIMENTAL SECTION

Materials. The synthesis of cryptophane-D has been first reported by Collet and co-workers in 1984.[24] Herein, cryptophane-D was synthesized using scandium triflate as catalyst and the procedure described by Brotin et al.[2] ^{13}C-labeled chloroform, dichloromethane, and the deuterated solvent 1,1,2,2-tetrachloroethane-d_2 were obtained from Cambridge Isotope Laboratory. The nonlabeled dichloromethane was obtained from Scharlau Chemie S.A and the nonlabeled chloroform from VWR. Because the cryptophane-D might have contained unknown amounts of molecular guests, a multistep procedure was applied in order to produce samples with accurately defined composition. This sample preparation procedure is different from that used in earlier work from our laboratories.[11,12] The cryptophane-D was first dissolved in nonlabeled dichloromethane and was left to dry in order to remove residual chloroform and other possible guests coming from synthesis. This step was repeated four times. The cryptophane-D was then dissolved in 1,1,2,2-tetrachloroethane-d_2 with help of an ultrasonic bath containing 40−50 °C warm water in order to remove as much of residual dichloromethane as possible. Subsequent analysis has shown, however, that dichloromethane that filled the cryptophane-D cavity cannot be removed in this way and resulting samples contained 65−75 mol % of dichloromethane with respect to concentration of cryptophane-D. Several samples with various compositions for different stages of the study were prepared, always with 1,1,2,2-tetrachloroethane-d_2 as solvent

(1) 35 mM cryptophane-D
(2) 11 mM cryptophane-D with 88 mM nonlabeled dichloromethane
(3) 10 mM cryptophane-D with 10, 23, 47, and 90 mM nonlabeled chloroform
(4) 11 mM cryptophane-D, 46 mM ^{13}C chloroform for guest exchange and relaxation measurements
(5) 11 mM cryptophane-D, 16 mM nonlabeled $CHCl_3$; chloroform was used in the preparation of this sample according to procedure described above instead of dichloromethane

NMR Spectra. ^{1}H and ^{13}C spectra were recorded with Bruker Avance spectrometers operating at 9.4, 14.1, and 16.5 T using 5 mm (BBI and BBO at 9.4 T, TXI at 14.1 T and cryo-TXI at 16.5 T) probe-heads. At 9.4 T the temperature calibration was done using standard methanol calibration sample, whereas a copper wire dipped into silicon oil contained in a 5 mm NMR tube was used at the two higher fields. The accuracy of the temperature determination is estimated at ±1 K. All of the experiments were repeated at least twice. The assignment was based on DQF-COSY,[25] (2D) NOESY, (2D) ROESY as well as ^{1}H-^{13}C edited HSQC[26−31] and HMBC[32] experiments.

The EXSY measurements were performed in the temperature range of 280−320 K at two fields (14.1 and 16.5 T) using the DPFGSENOE sequence with two selectively refocusing shaped pulses and one hard π pulse in the middle of the mixing time interval.[33] The semi-selective inversion pulses were implemented as Gaussian G3 cascades[34] with the duration of 20 ms. The hard ^{1}H $\pi/2$ pulse was between 8 and 10 μs. Sixteen different build up time intervals were used. Experiments were performed with 64 accumulated signal transients, using relaxation delay of 35 s. Only the doublets of the ^{13}C -labeled chloroform were evaluated. The purpose of the label is to enhance the proton spin−lattice relaxation. The evaluation of the exchange rate of the decomplexation reaction (k_{bf}) was based on the approach proposed originally by Macura et al.[35] and described by Hu and Krishnamurthy.[36] The determination of the exchange rate of the forward reaction (k_{fb}) was based on the principle of detailed balance, in order to avoid the error coming from small intensities at very short mixing times in the initial rate regime.

The same approach was used to measure the cross relaxation rates in the laboratory (σ^{NOE}) and in the rotating frame (σ^{ROE}). The mixing times were in the range from 0.05 to 0.5 s for the laboratory frame cross-relaxation. The rotating frame cross-relaxation was only measured at 16.5 T and the length of the spin lock was varied between 0.05 and 0.2 s using a spin lock field of 2.9 kHz.

^{13}C spectra were recorded with Waltz16 at 9.4 T, Waltz65 at 14.1 T and biwaltz256[37] at 16.5 T proton decoupling. At the two higher fields, the decoupling sidebands of the ^{13}C-labeled chloroform signal were visible when the waltz16 composite pulse was used, and these were removed by the two other composite pulse sequences. The hard $\pi/2$ pulse was between 5.7 and 9 μs, depending on the field and temperature used and the decoupler $\pi/2$ pulse was between 80 and 100 μs. The ^{13}C spin−lattice relaxation times were measured by the inversion−recovery method using 16 recovery delays from 0.5 ms to $5T_1$. The relaxation delay was set to $6T_1$. The spin−lattice relaxation times of the labeled chloroform were measured by using 128 accumulated scans. In the case of the host, having much shorter relaxation times, 512 to 1024 scans were used in order to get the desired signal-to-noise ratio. The nuclear Overhauser enhancement was measured with the dynamic NOE

dx.doi.org/10.1021/jp303469x | J. Phys. Chem. B 2012, 116, 7898−7913

sequence.[38] The NOE build-up delay was set to $5T_1$ and the relaxation delay to $10T_1$. In the spectrum with no NOE enhancement, the build-up delay was set to 0.1 ms.

Quantum Chemical Calculations. All calculations were performed using the Gaussian 09 package.[39] Geometries were optimized on the level of DFT-B3LYP functional with the basis set 6-31G(d). The optimized structure was then taken, and a single-point energy calculation was done, together with the calculation of the ^{13}C chemical shift using the GIAO method[40] with the basis set 6-311+G(2d,p). All of the calculations were performed in dichloroethane solvent using the conductor polarizable continuum model (CPCM).[41,42] Two sets of calculations were made: one for the empty host and one with a chloroform molecule inside the cavity. The van der Waals interaction was taken into consideration in all structures optimized with the B3LYP functional by adding the empirical term to the DFT energies.[43] The lowest energy conformers from B3LYP calculations in the case of chloroform-containing host were reoptimized with the B97D functional, as it was described by Grimme et al.[43]

RESULTS

Conformational Flexibility of Cryptophane-D. *Quantum Chemical Calculations.* Cryptophane-D molecule contains flexible parts such as three ethylenedioxy linkers and methoxy groups that can adopt different conformations in solution. We performed an extensive set of quantum chemical calculations using DFT in order to obtain geometries, energies and carbon-13 chemical shifts of the conformers that can be populated in our NMR samples. Each of the ethylenedioxy linkers can occur in two nonequivalent trans and four gauche rotameric states. The two trans geometries differ in the relative orientation of the linker carbons compared to the oxygens (T_1 and T_2 see Figure 1). The four gauche conformers differ in the sign of the dihedral angle (+60° or −60°) and in the relative orientation compared to the oxygens ($G_{\mp,1/2}$), similarly to trans conformers. The numbering 1 and 2 denotes the relative position of the carbon 2′. Index 1 corresponds to the carbon "pointing" toward the methoxy group and index 2 denotes the opposite geometry with the carbon oriented away from the methoxy group. The most stretched structure is the $T_2T_2T_2$ conformer with the distance between the carbons B and B″ of 10 Å, which is somewhat longer than 9.6 Å in the $T_1T_1T_1$. The least stretched structures are $G_{+2}G_{+2}G_{+2}$ and $G_{-2}G_{-2}G_{-2}$. The distances between the carbons B and B″ in these structures are 8.9 and 9 Å, respectively. The B to B″ distance is not unique for the mixed conformers containing linkers in both conformations *G* and *T*, and it varies between 8.8 and 10 Å making these conformers asymmetric.

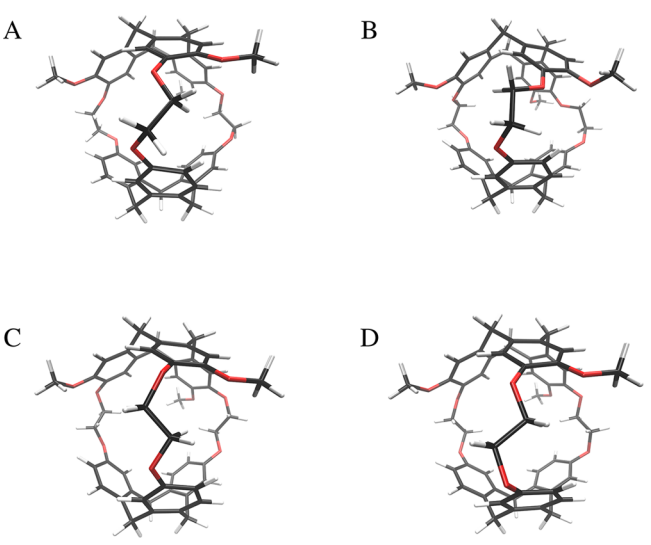

Figure 1. Some of the possible conformers of cryptophane-D: (A) is the $G_{+1}G_{+1}G_{+1}$, (B) is the $G_{-2}G_{-2}G_{-2}$, (C) is the $T_2T_2T_2$, and (D) is the $T_1T_1T_1$ conformer.

There is a total number of 56 relevant conformers when considering different combination of linkers rotameric states. They can be divided into four groups: *TTT* (4 conformers), *GTT* (12 conformers), *GGT* (20 conformers), and *GGG* (20 conformers). We selected the 22 most representative structures out of them for the quantum chemical calculations of the guest-free host. The DFT calculations show that the rotamers with index 2 have always lower energies than the corresponding rotamer denoted with index 1. Thus, $G_{-2}G_{-2}T_2$ is lower in energy than $G_{-2}G_{-2}T_1$. The obtained total energy was utilized to calculate the Boltzmann distribution of populations of conformers at 298 K. Degeneracy factor 3 was used for the structures with two linkers adopting identical conformation, and degeneracy factor of 1 for the structures with all three linkers with the same geometry (Figure 2). It should be noted here that the presented population distribution is only semiquantitative as it is calculated from an incomplete set of structures. Table of the full results of the quantum chemical calculations for 22 conformers, including different contributions to the total energies (the electronic energy, the zero-point correction, the thermal contributions, and the van der Waals interaction energy[43,44]) is provided as Supporting Information.

We also calculated ^{13}C chemical shifts for all optimized structures. Among them, the shifts of the nuclei C1′ and C2′ display the largest variability with respect to the different conformations of the linkers. The calculated difference ($\delta_{2'} - \delta_{1'}$) is the largest and positive in the case of $G_{-2}G_{-2}G_{-2}$ (4.7 ppm) and $T_2T_2T_2$ (6.8 ppm) conformers. This difference is negative in the case of $T_1T_1T_1$ (−4.7 ppm) and $G_{+2}G_{+2}G_{+2}$ (−3.8 ppm). Conformers containing linkers G_{+2} and T_1 have smaller or negative ($\delta_{2'} - \delta_{1'}$) value. A complete summary of the calculated chemical shifts is provided in the Supporting Information. Some of the possible conformations of cryptophane-D are shown in Figure 1.

Having the DFT optimized atomic coordinates for various conformers, one can estimate the corresponding cavity volumes. We do this in two ways. In the first approach, we place van der Waals spheres on each atom in the molecule. Then, we insert a test sphere inside the cavity and let its radius grow until it touches any of the atomic van der Waals spheres in the cavity walls. We move the center of the test sphere to obtain as large radius as possible for a given cavity geometry. The test sphere volumes, which can be treated as lower bounds to the real cavity volume, for selected conformers are listed in Table 1. In the second approach, we estimate the cavity volume using the Voidoo software.[45−48] The volumes obtained in this way are also given in Table 1. They should be larger than obtained in the first approach, which indeed is the case. We may notice that the difference between the two volumes is large in some conformers, e.g., in the elongated $T_1T_1T_1$ or $T_2T_2T_2$, while it is quite small for others, characterized by a more sphere-like cavity shape (e.g., $G_{-1}G_{-1}G_{-1}$).

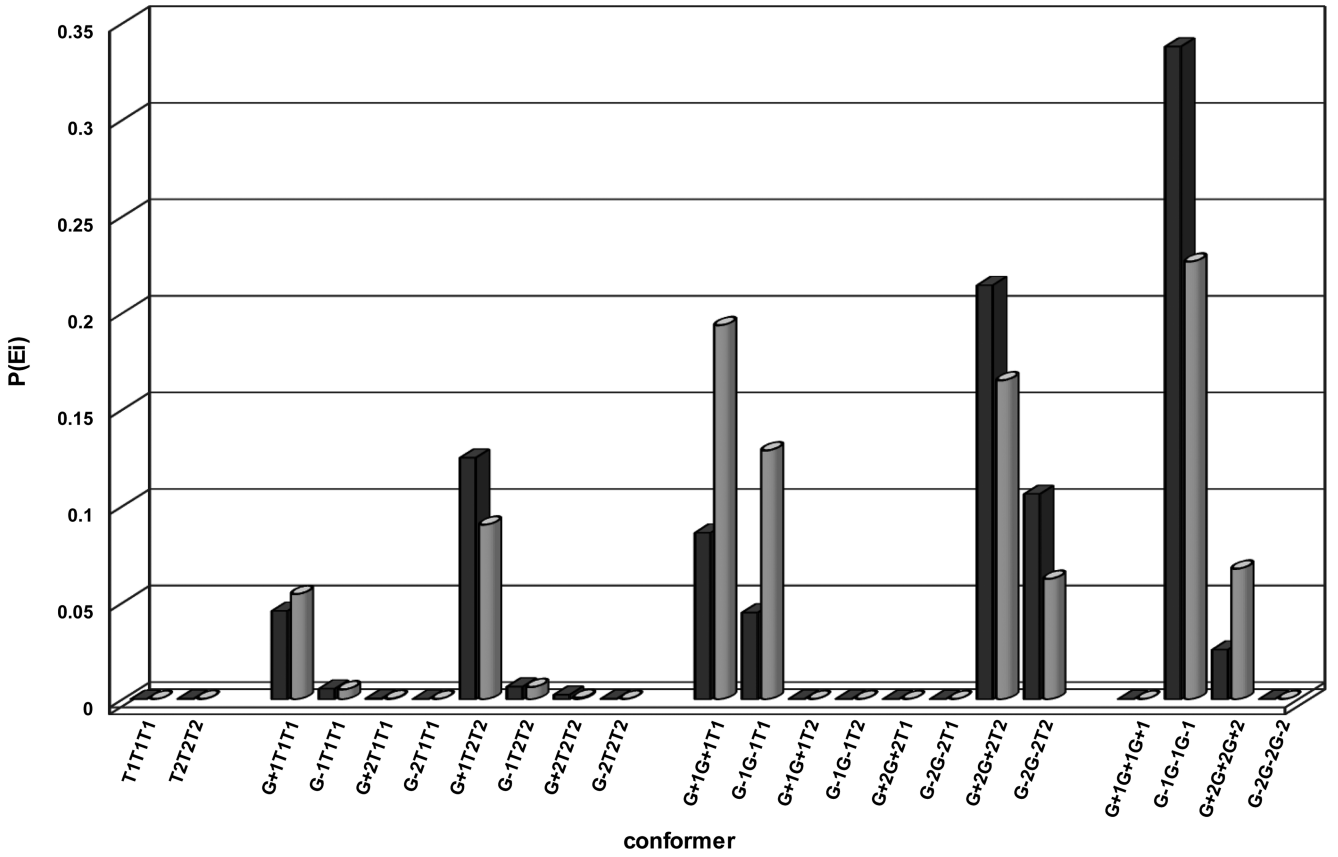

Figure 2. Boltzmann distribution of the calculated conformers for cryptophane-D without guest. The black box denotes the basis set 6-31G(d) (optimization) and the gray cylinder the 6-311G+(2d,p) (single-point). The energies include the zero-point, thermal and van der Waals corrections. The degeneracy factor is included.

Table 1. Estimated Volumes of the Cavities of Different Conformers[a]

conformer	V_1 (Å^3)	V_2 (Å^3)
$T_1T_1T_1$	59	147 (1.2)
$T_2T_2T_2$	85	160 (1.4)
$G_{+1}T_1T_1$	61	98 (1.2)
$G_{+1}T_2T_2$	69	83 (1.4)
$G_{+1}G_{+1}T_1$	57	81 (1.4)
$G_{-1}G_{-1}T_1$	34	46 (1.2)
$G_{+1}G_{+1}T_2$	58	85 (1.2)
$G_{-2}G_{-2}T_2$	51	79 (1.2)
$G_{-2}G_{-2}G_{-2}$	55	91 (1.4)
$G_{-1}G_{-1}G_{-1}$	75	81 (1.2)
$G_{+2}G_{+2}G_{+2}$	47	87 (1.4)

[a] V_1 denotes the volume of the biggest test sphere which fits into the cavity. V_2 denotes the estimated cavity volumes by the software Voidoo.[45−48] The number in brackets is the probe radius used for the volume estimation in Å. For the calculation the van der Waals radii were 1.2 Å for H, 1.7 Å C, and 1.52 Å for O.

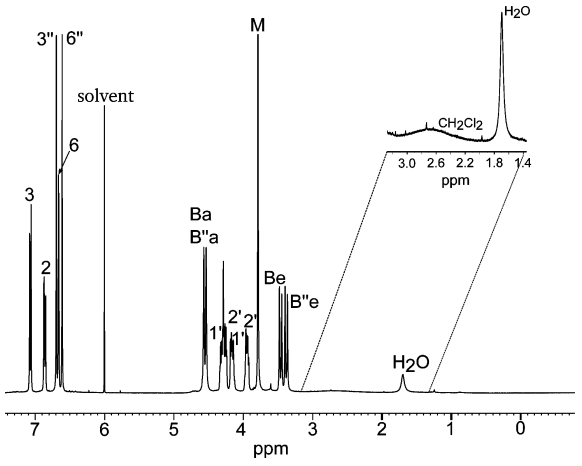

Figure 3. ^{1}H spectrum of 35 mM cryptophane-D solution in 1,1,2,2-tetrachloroethane-d_2 solvent at 280 K and 400 MHz.

NMR Spectra. The ^{1}H (at 400 MHz) and ^{13}C spectra (150 MHz) of 35 mM cryptophane-D solution at 280 K are shown in Figures 3 and 4, respectively, together with signal assignments.

Despite our substantial effort (see Materials section), we were not able to obtain a sample of cryptophane-D host free of any potential guests. Thus, the NMR spectra of 35 mM cryptophane-D dissolved in 1,1,2,2-tetrachloroethane-d_2 contain a single set of peaks from all nuclei of the host, a peak from water and a substantially broadened and chemical-exchange-shifted peak from CH_2Cl_2 (Figures 3 and 4). Recording the spectrum at low temperature, where the exchange is slowed down, allowed to determine the concentration of dichloromethane as about 65% of the total concentration of the host. Clearly, the empty cavity of cryptophane-D is a strongly disfavored situation ("horror vacui") and the guest molecule is kept included in the cavity very strongly when the concentration of potential guests in solution is low. It turns out that the best NMR spectra of empty host have been

dx.doi.org/10.1021/jp303469x | J. Phys. Chem. B 2012, 116, 7898−7913

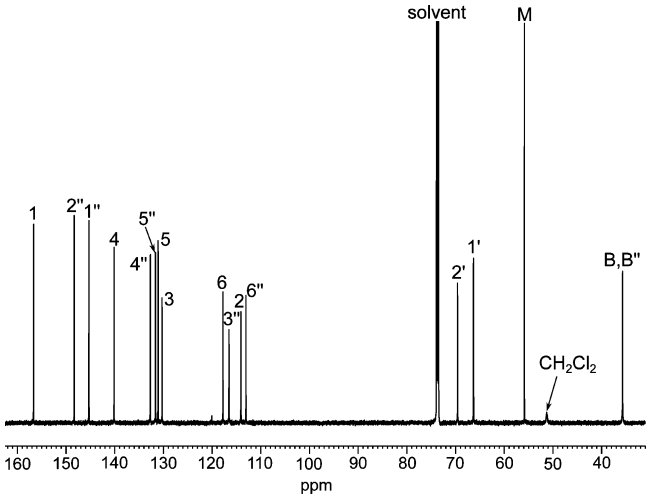

Figure 4. ^{13}C spectrum of 35 mM cryptophane-D solution in 1,1,2,2-tetrachloroethane-d_2 solvent at 280 K and 150 MHz.

achieved from the sample containing 11 mM cryptophane-D and 16 mM chloroform (item no. 5 of list of samples in the Material section), in which we succeeded to remove dichloromethane quantitatively. Because there is a slow exchange between peaks of free and complexed host, this sample provides also a reasonably well separated spectrum of the free cryptophane-D (see Figure 10c below). The chemical shift difference $\delta_{2'}-\delta_{1'}$ in the ^{13}C spectrum that is characteristic for the conformation of the linkers is 1.3 ppm, which is in very good agreement with the calculated population-weighted chemical shift difference that is −0.3 ppm or 0.9 ppm for the low and for the high basis set, respectively.

Dynamics of the Host. A solution containing 35 mM of cryptophane-D was also used to study carbon-13 relaxation of the host at natural abundance in order to assess conformational dynamics that takes place in subnanosecond time-scale. The longitudinal relaxation rate and the heteronuclear NOE was measured for all the carbons at three fields (9.4, 14.1, and 16.5 T) by directly detected inversion−recovery method.

The molecule is medium-sized and the longitudinal relaxation is field dependent. From a relaxation point of view we can divide the carbons into groups with different number of directly bound protons, mobility and hybridization. The aromatic (sp^2) carbons not having any protons attached (4, 5, 1, 1″, 2″, 4″, and 5″) will have the chemical shift anisotropy (CSA) as the main relaxation mechanism and the DD interaction with protons nearby as a small contribution. Carbons of this type have been used to obtain information about distances to incorporated guests,[49] but we do not find this strategy possible to apply here for sensitivity reasons. The aromatic carbons with protons attached (2, 3, 6, 3″, and 6″) will have the dipolar coupling to the proton and CSA as main relaxation mechanisms. Among the nonaromatic (sp^3) carbons three groups can be distinguished. The carbons in the linkers between the two caps (1′ and 2′), the bridging carbons between the phenyl groups (B and B″) and the methyl groups. The main relaxation mechanism for all these carbons is the dipolar coupling to the attached protons while CSA contribution was neglected. The measured values for the carbons carrying attached protons are shown in Table 2.

The relaxation data have been interpreted by means of the Lipari−Szabo "model-free" approach (eq 15). The same DCC value was used for all of the proton-bearing carbons, based on the CH bond length of 1.091 Å. In order to include also the aromatic carbon sites, we calculated the anisotropy of the chemical shielding tensor ($\Delta\sigma$) using the DFT-GIAO method. The obtained average value of 140 ppm was used in the analysis of relaxation data. The truncated Lipari−Szabo model was found sufficient for the proton carrying aromatic carbons (eq 16). The aromatic carbons without any directly attached protons were not included into analysis due to relatively large uncertainty of the value of the CSA. The global correlation time and the parameters of internal motions for all proton carrying carbons are summarized in Table 3. The generalized order parameter of the nuclei of the aromatic rings and the bridges close to 1 documents the high rigidity of CTB units. The experiment confirmed that the parts introducing some internal flexibility into cryptophane-D molecule are the linkers (C1′, C2′, S^2 = 0.55) and the methyl groups that undergo nearly unrestricted rotational diffusion (S^2 = 0.08).

Table 2. ^{13}C Relaxation Data of Cryptophane-D without Guest at 280 K

	field					
	9.4 T		14.1 T		16.5 T	
^{13}C site	R1(s^{-1})	NOE	R1(s^{-1})	NOE	R1(s^{-1})	NOE
2, 3, 6, 3″, and 6″	6.2	1.49	5.2	1.27	4.8	1.21
2′ and 1′	7.0	1.82	5.3	1.63	4.6	1.53
$-OCH_3$	1.74	2.02	1.54	1.95	1.49	1.95
B and B″	9.8	1.60	6.9	1.37	5.8	1.34

Table 3. Motional Parameters of Cryptophane-D at 280 K[a]

^{13}C site	S^2	τ_{loc} (ps)
2, 3, 6, 3″, and 6″	0.97 (0.07)	
1′ and 2′	0.55 (0.01)	50 (30)
$-OCH_3$	0.08 (0.01)	10 (4)
B and B″	0.83 (0.13)	
τ_{global} (ps)	830 (81)	

[a]The error was calculated by the Monte Carlo method and is given as standard deviation.

Cryptophane-D−Dicholoromethane System. In order to experimentally investigate dynamics of the cryptophane-D−dichloromethane system, we employed the sample with a large excess of dichloromethane in order to maximize concentration of the complex. Variable temperature ^1H and ^{13}C spectra were recorded between 230 and 300 K. The proton spectra are shown in Figure 5, and the ^{13}C spectra of the aliphatic region are shown in Figure 6. There is only one set of peaks of the host in the whole temperature range; that is, the free and bound states of the host are in fast chemical exchange. In Figure 5 one can see slight chemical shift and full width at half height change of the host peaks. This is due to the Boltzmann distribution of complexed dichloromethane conformations changing with temperature. Conversely, dichloromethane displays slow chemical exchange between the free and bound states in the ^1H spectrum at 230 K. At higher temperatures coalescence occurs and a single peak due to fast exchange is observed at 300 K. The exchange rates determined by line-shape fitting, cf. Table 4, fall in the range 14−5300 s^{-1} and 100−44000 s^{-1} for k_{fb} and k_{bf}, respectively. The Arrhenius activation energies for both processes are 49 and 50 kJmol^{-1}, respectively. The ratio

dx.doi.org/10.1021/jp303469x | J. Phys. Chem. B 2012, 116, 7898−7913

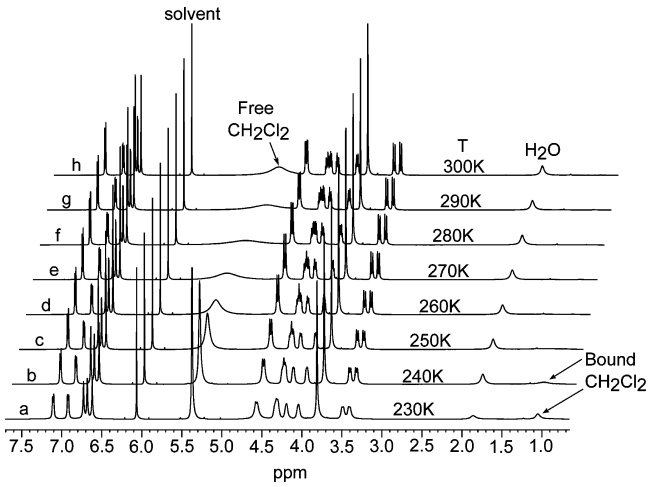

Figure 5. Variable temperature ^{1}H spectrum at 600 MHz of the solution containing 11 mM cryptophane-D and 88 mM CH_2Cl_2 with 1,1,2,2-tetracholroethane-d_2 as a solvent. (a) 230, (b) 240, (c) 250, (d) 260, (e) 270, (f), 280, (g) 290, and (h) 300 K.

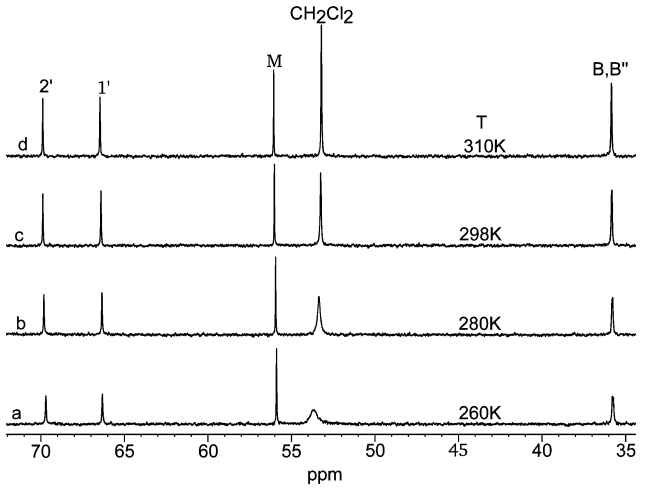

Figure 6. Variable temperature ^{13}C spectrum at 100 MHz of the solution containing 11 mM cryptophane-D and 88 mM CH_2Cl_2 with 1,1,2,2-tetracholroethane-d_2 as a solvent. (a) 260, (b) 280, (c) 298, and (d) 310 K.

Table 4. Results of Line-Shape-Fitting for the Cryptophane-D + CH_2Cl_2 System

T (K)	p_f	p_b	k_{fb} [s^{-1}]	k_{bf} [s^{-1}]
230	0.877	0.123	14	98
240	0.874	0.126	43	300
250	0.872	0.128	109	750
260	0.870	0.130	265	1800
270	0.880	0.120	580	4300
280	0.887	0.113	1300	10 300
290	0.889	0.111	2700	22 000
300	0.891	0.109	5300	44 000

k_{fb}/k_{bf} (or p_b/p_f) is only weakly dependent on temperature over the whole interval.

The error analysis of the data indicates that the k_{fb} rate is always quite well determined, with an uncertainty of less than 10%. Also the relative population of the free site, p_f, is reasonably trustworthy, in particular when the coalesced line is quite narrow. The uncertainties in k_{fb} and p_f propagate into p_b and k_{bf}. These uncertainties, together with the low (and thus highly error-prone) concentration of the free host, make the data inappropriate for quantitative determination of the equilibrium constant. Qualitatively, the equilibrium constant seems to be weakly temperature dependent which indicates a low complexation enthalpy, in agreement with the fact that the two activation energies acquire similar values.[50] As a consequence, the complex formation appears to be driven by a positive complexation entropy.

Cryptophane-D−Chloroform System. *Equilibria and Kinetics of Complex Formation.* Addition of excess of chloroform leads to doubling the number peaks of the host in the NMR spectra (Figures 7 and 8). The strongly shielded

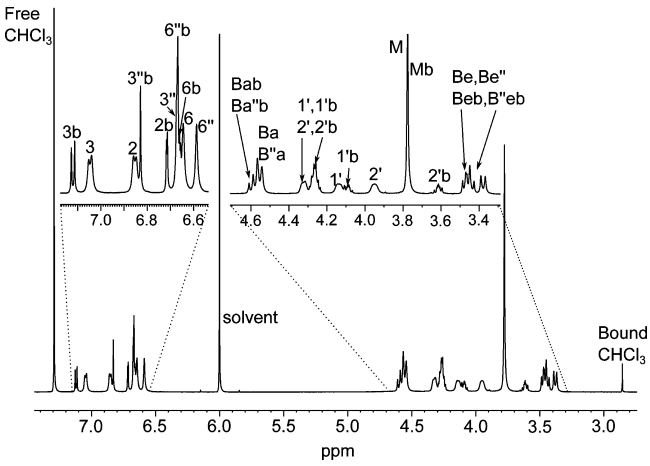

Figure 7. ^{1}H spectrum of 10 mM cryptophane-D solution with 47 mM nonlabeled $CHCl_3$ with 1,1,2,2-tetrachloroethane-d_2 as a solvent at 280 K and 600 MHz. The letter "b" after the assignment denotes chloroform-containing host.

peak of chloroform guest included in the cryptophane-D cavity appears at 2.9 ppm in the ^{1}H spectrum and at 74.3 ppm in the ^{13}C spectrum. The peaks of the free chloroform are at their "ordinary" chemical shifts providing the complexation shifts as large as 4.3 ppm and 3 ppm for the ^{1}H and ^{13}C spectrum, respectively. Clearly, chemical exchange for the host as well as

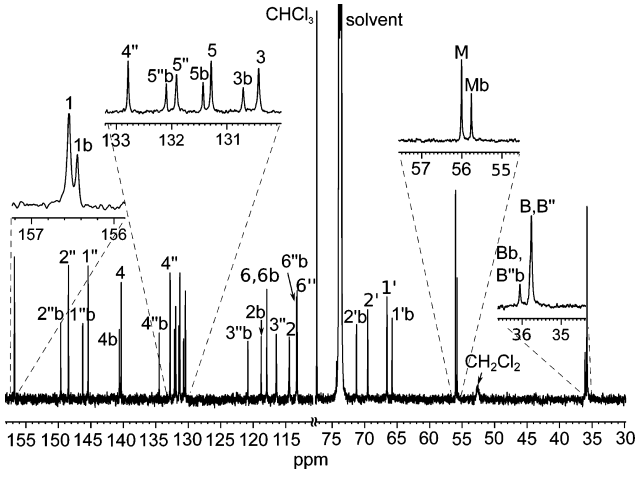

Figure 8. ^{13}C spectrum of 10 mM cryptophane-D solution with 47 mM nonlabeled $CHCl_3$ with 1,1,2,2-tetrachloroethane-d_2 as a solvent at 280 K and 150 MHz. The letter "b" after the assignment denotes chloroform-containing host.

dx.doi.org/10.1021/jp303469x | J. Phys. Chem. B 2012, 116, 7898−7913

the guest is in the slow regime in both ^{1}H and ^{13}C spectra (at 600 and 150 MHz respectively, 280 K). The peak of the bound chloroform appears at 74.3 ppm; although it is weak at natural isotopic abundance, it is more apparent in the spectrum from the sample with ^{13}C -labeled chloroform (Figure 9).

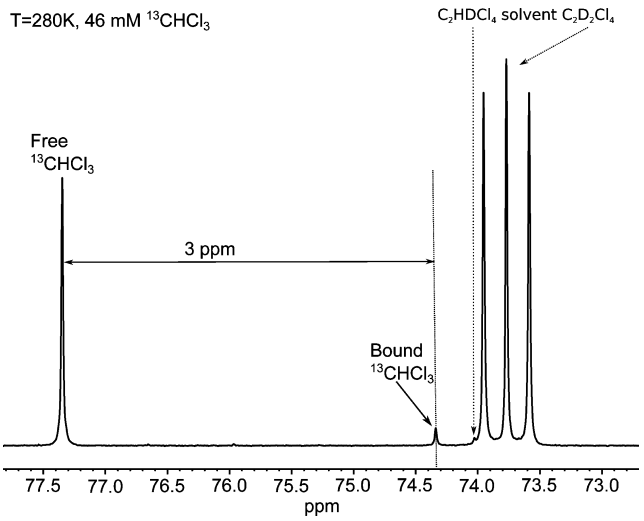

Figure 9. ^{13}C spectrum of 11 mM cryptophane-D with 46 mM ^{13}C labeled $CHCl_3$ with 1,1,2,2-tetrachloroethane-d_2 as a solvent at 280 K and 150 MHz.

With the methods described in the Materials section (samples 1−4), we were not able to remove all of the dichloromethane during the sample preparation procedure. Consequently, the samples with excess of chloroform still contained small amount of dichloromethane. Such sample composition seems quite complicated. However, the different regime of chemical exchange due to complexation of chloroform (slow) and dichloromethane (fast) allows the isolation of the spectrum of cryptophane-D−chloroform complex, thus enabling investigation of its physicochemical properties. This is best demonstrated in the region of the ^{13}C spectra corresponding to the nuclei of the linkers, 1′ and 2′ (65−72 ppm). The spectra of three samples that differ in composition are shown in Figure 10. The lines originating from cryptophane-D - chloroform complex are the two outer lines (1′ at 65.8 ppm and 2′ at 71.3 ppm) and they do not shift with concentration. On the other hand, the remaining species of cryptophane-D: free cryptophane-D and cryptophane-D complex with dichloromethane are in fast mutual exchange and, consequently, the positions of the corresponding lines ("inner" lines in Figure 10) strongly depend on the concentration of dichloromethane.

Thus, analyzing the ^{1}H and ^{13}C spectra of the sample series containing a fixed concentration of cryptophane-D (10 mM) and varying concentrations of chloroform (10−90 mM) at 280 K (see the Supporting Information for the spectra), we could calculate the stability constant of K = 12.1 M and the concentrations of the components as shown in Figure 11 by means of eqs 1 and 4. We should note here that the symbol [H] means the concentration of CH_2Cl_2@cryptophane−D complex rather than the concentration of the free host, and the value of the equilibrium constant is specific for the presence of dichloromethane in the sample. Figure 11 shows that a large excess of chloroform (9:1) is required to achieve roughly 50% filling of the cryptophane-D with chloroform.

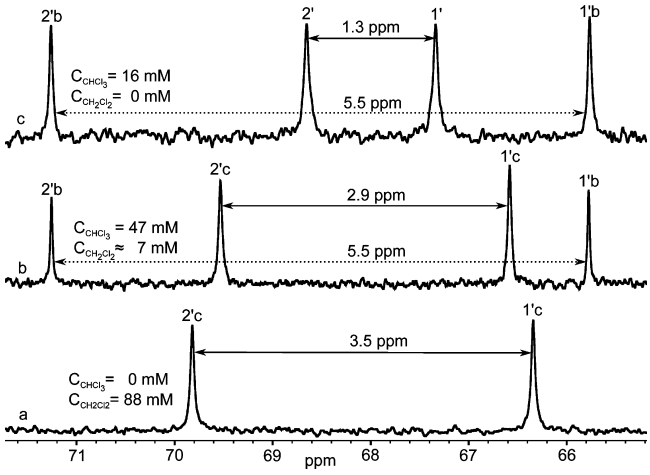

Figure 10. Comparison of the linker region in the ^{13}C spectra of three different solutions with 1,1,2,2-tetracholroethane-d_2 as a solvent. Spectrum "a" corresponds to the solution with 11 mM cryptophane-D and 70 mM CH_2Cl_2, spectrum "b" to the solution containing 10 mM cryptophane-D, 47 mM of nonlabeled $CHCl_3$ and a small amount of CH_2Cl_2 and spectrum "c" to the solution with 10 mM cryptophane-D and 16 mM nonlabeled $CHCl_3$. Spectrum "b" was taken at 150 MHz and "a" and "c" were taken at 100 MHz. All of the spectra were recorded at 280K. The letter "c" in the assignment denotes the peaks belonging to the CH_2Cl_2 complex.

Next, we acquired temperature dependent spectra of the cryptophane-D−chloroform system (the sample containing 10 mM cryptophane-D and 46 mM chloroform) in the range of 240−298 K (^{1}H and ^{13}C spectra are shown in Figures 12−14). The free and bound chloroform peaks remain in slow exchange throughout the whole temperature range. The carbon-13 signals from the chloroform-containing and the chloroform-free form of the host show different behavior at low temperatures, as can be seen most clearly in Figure 13. The lines corresponding to the host without chloroform display significant exchange broadening, while the lines of the chloroform-containing species remain narrow. The reason for this difference is related to the presence of a small amount of dichloromethane in our samples and the broadening is an indication of the exchange between empty and dichloromethane-containing host. Thus the smaller guest allows for more conformational freedom of the linkers.

The reaction rate of the decomplexation reaction was measured at three temperatures, 280, 295, and 320 K, using the 1D EXSY method. Only the solution containing 10 mM cryptophane-D and 46 mM ^{13}C labeled chloroform was used, in order to avoid the complications caused by inconveniently slow relaxation of the chloroform protons in the unlabeled species. The build-up curves are shown in Figure 15. The error of the build-up rates is 10−15%. The rate of the "forward" complexation reaction was then obtained from the principle of detailed balance, making use of the equilibrium constants from the integrals of the free and bound chloroform peaks of the proton spectra at the same temperatures. The results are shown in Table 5.

From the temperature dependence of the equilibrium constant, we can estimate the enthalpy (ΔH^0) and entropy (ΔS^0) of the complex formation. The enthalpy is −17 kJ mol^{-1} and the entropy is −38 J mol^{-1} K^{-1}. The fact that both values are negative can be associated with the enthalpy−entropy compensation.[51] The activation energies of the forward and

dx.doi.org/10.1021/jp303469x | J. Phys. Chem. B 2012, 116, 7898−7913

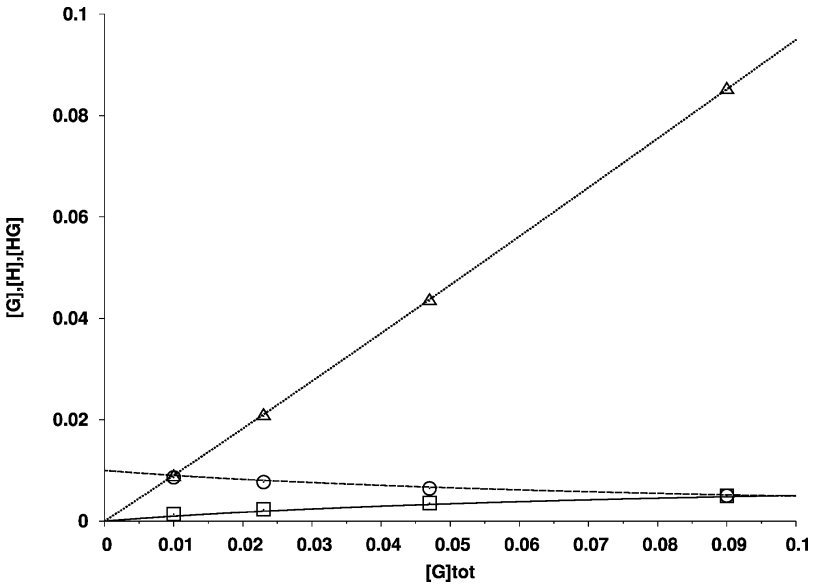

Figure 11. Distribution diagram of species in equilibrium in solutions of 10 mM cryptophane-D with different concentration of nonlabeled $CHCl_3$ at 280 K. The lines are calculated according to eq 4 for K = 12.1. The dashed line represents the free host [H], the dotted line the free guest [G], and the solid line the complex [HG] concentration. The points represent the four solutions. ⊙, ⊡, and Δ depict the determined concentration of [H], [HG], and [G], respectively.

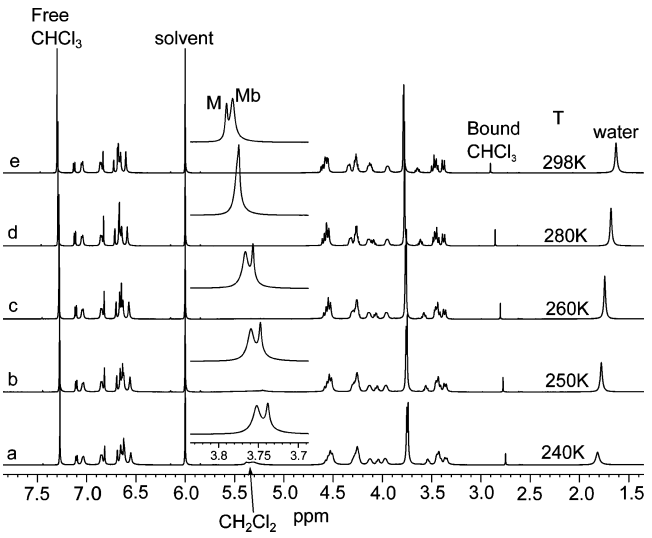

Figure 12. ^{1}H variable temperature spectra at 600 MHz of 10 mM cryptophane-D solution with 47 mM nonlabeled $CHCl_3$ with 1,1,2,2-tetracholroethane-d_2 as solvent. The temperature increases going from a to e and is, respectively, 240, 250, 260, 280, and 298 K.

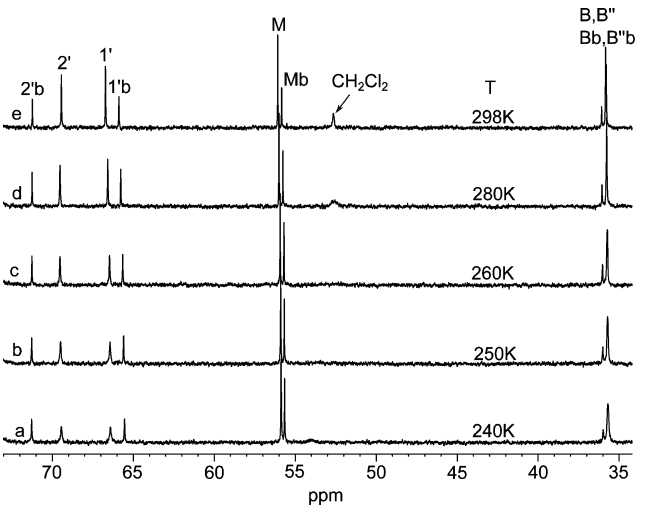

Figure 13. ^{13}C variable temperature spectra at 150 MHz of aliphatic region of 10 mM cryptophane-D solution with 46 mM nonlabeled $CHCl_3$ with 1,1,2,2-tetracholroethane-d_2 as solvent. The temperature increases going from a to e and is, respectively, 240, 250, 260, 280, and 298 K.

backward complexation reactions can be determined from the Arrhenius equation. We found that the complexation reaction has an activation energy of 47 kJ mol^{-1} and the value for the opposite process is 63 kJ mol^{-1}. We can notice that the reaction enthalpy agrees well with the difference between the activation energies of the forward and backward reactions, a phenomenon noticed earlier in the study of the host–guest complexes of cryptophane-E.[50]

Structure of the Cryptophane-D–Chloroform Complex. Structural aspects of the complex formed between cryptophane-D and chloroform were addressed experimentally by means of 2D NOESY and series of selective 1D NOE and ROE measurements. The relevant part of the 2D NOESY spectrum is shown in Figure 16. Major cross-peaks arise from the mutual dipolar interactions of ^{1}H nuclei within the host molecule which were used for spectral assignment. There is also a set of cross-peaks between the bound guest and the aromatic protons of cryptophane-D, whereas there are no cross-peaks from the free guest except the one due to chemical exchange between the free and bound guest as described in the preceding section. The quantitative 1D NOE and ROE were used to determine whether there is a preferential orientation of chloroform guest inside of the host consisting of two different hemispheres. The determined cross-relaxation rates between the bound guest and the aromatic protons of the both hemispheres are very similar (see Table 6). The cross-relaxation rate is a very sensitive measure of internuclear distance since it is inversely proportional to the sixth power of the distance. Due to the similarity

dx.doi.org/10.1021/jp303469x | J. Phys. Chem. B 2012, 116, 7898–7913

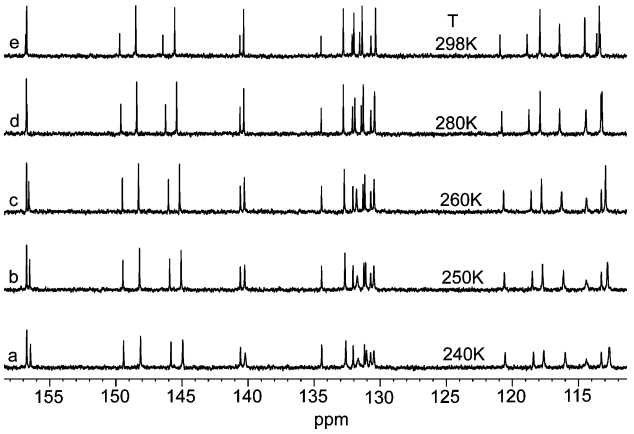

Figure 14. ^{13}C variable temperature spectra at 150 MHz of phenyl region of 10 mM cryptophane-D solution with 46 mM nonlabeled $CHCl_3$ with 1,1,2,2-tetracholroethane-d_2 as solvent. The temperature increases going from a to e and is, respectively, 240, 250, 260, 280, and 298 K.

of the cross-relaxation rates for nuclei of the both hemispheres it is evident that there is no significant preference in the orientation of the C−H bond of chloroform for any of the two hemispheres. This finding contrasts with our previous measurements of cross relaxation in the complex of cryptophane-C (which is the structural isomer (anti) of cryptophane-D) and chloroform.[9]

In order to attain a more detailed view of the structural aspects, such as the orientation of the chloroform guest inside of the cavity and the conformational preferences of the chloroform-containing cryptophane-D, we carried out an extensive set of DFT calculations. We used a similar strategy as for the empty host, but some of the low-energy conformers were reoptimized with B97D functional[43] in order to include better the van der Waals interaction into the optimization. The results are shown in Table 7 and in the Supporting Information.

Table 5. Equilibrium and Kinetic Data, where the Total Concentration of Cryptophane-D is 10 mM

T [K]	k_{fb} [s^{-1}]	k_{bf} [s^{-1}]	[H] [mM]	K [M^{-1}]
280	0.02	0.25	6.6	12.1
295	0.06	0.82	7.1	10.0
320	0.30	7.24	8.2	5.1

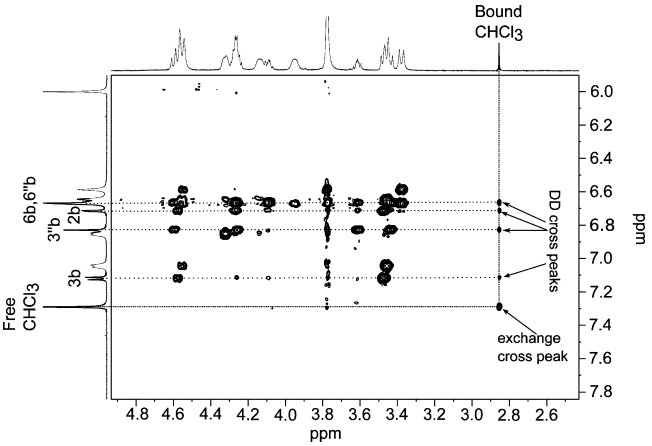

Figure 16. Part of ^1H-^1H 2D NOESY spectrum of 10 mM cryptophane-D solution with 47 mM nonlabeled $CHCl_3$ with 1,1,2,2-tetracholroethane-d_2 as solvent at 280 K at 600 MHz with a mixing time of 0.2 s.

Table 6. ^1H Cross-Relaxation Rates between the Guest and Host at 280 K

^1H	3″b	6b	2b
NOE	0.037	0.026	0.034
ROE	0.039	0.029	0.036

The calculated free energies of different conformations are found to depend heavily on the level of theory used. When

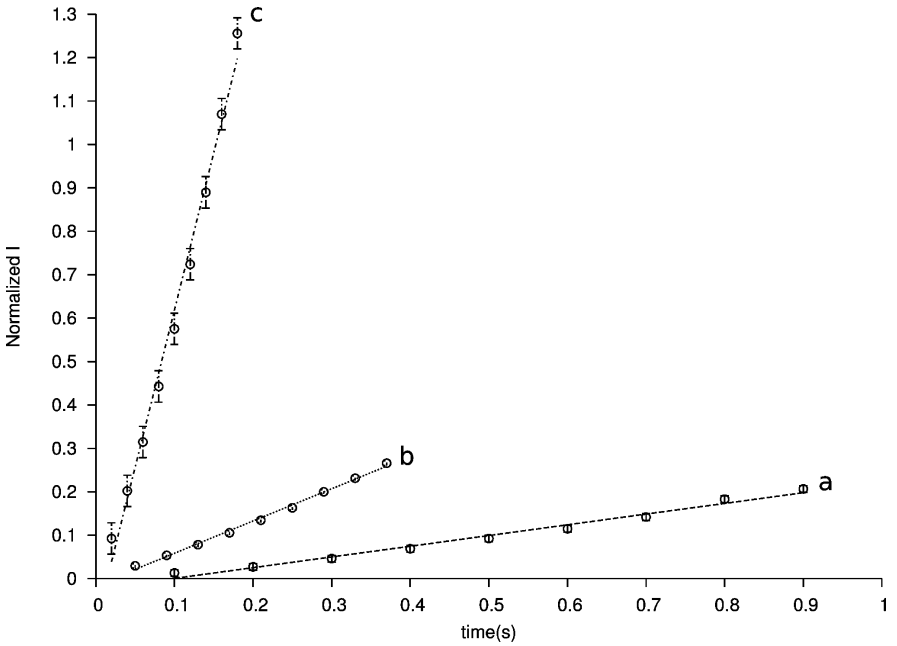

Figure 15. ^1H 1D EXSY of 10 mM cryptophane-D solution with 46 mM labeled $CHCl_3$ with 1,1,2,2-tetracholroethane-d_2 as solvent. (a) 285, (b) 295, and (c) 320 K. The error bars indicate the root-mean-square error from the trendline.

dx.doi.org/10.1021/jp303469x | J. Phys. Chem. B 2012, 116, 7898−7913

Table 7. Relative Energies of the Most Abundant Conformers Optimized with Different Functionals[a]

functional	B3LYP	B3LYP	B3LYP	B3LYP	B3LYP	B3LYP	B97D	B97D	B97D	B97D
conf./energy	e	ee	eee	E	EE	EEE	e	ee	E	EE
$T_2T_2T_2(1)$	0.0	0.0	0.8	0.0	0.0	6.2	3.5	0.0	9.2	0.0
$T_2T_2T_2(2)$	0.3	0.5	1.3	0.4	0.6	6.8	5.3	5.7	11.1	5.9
$G_{+2}T_2T_2(1)$	9.7	5.9	0.5	7.3	3.5	3.4	7.5	10.9	9.9	8.4
$G_{+2}T_2T_2(2)$	8.9	8.0	2.9	6.3	5.5	5.8	8.0	6.2	10.6	4.0
$G_{-2}T_2T_2(1)$	7.8	7.8	0.0	5.5	5.5	3.0	2.1	8.0	4.9	5.2
$G_{-2}T_2T_2(2)$	7.6	14.3	3.6	4.8	11.5	6.3	1.4	9.6	4.6	7.2
$G_{-2}G_{-2}T_2(1)$	16.9	19.1	3.2	12.1	14.3	3.8	0.7	8.5	1.3	3.5
$G_{-2}G_{-2}T_2(2)$	17.5	24.1	4.3	11.7	18.3	3.9	0.0	6.1	0.0	0.5
$G_{-2}G_{-2}G_{-2}(1)$	28.6	26.6	4.0	19.2	17.2	0.0	6.9	13.3	3.7	4.5
$G_{-2}G_{-2}G_{-2}(2)$	32.6	36.1	12.3	22.5	26.0	7.6	11.6	19.3	9.0	11.0

[a]e denotes only the electronic energy at the basis set 6-31G(d) and E at 6-311+G(d,p). EE and ee denote the electronic plus the zero-point correction plus the thermal contributions. EEE and eee contain also the van der Waals contributions. The number in brackets (1 or 2) denotes the orientation of chloroform. Number 1 means that the C−H bond points towards the cap with methoxy group on it, and number 2 denotes the opposite direction.

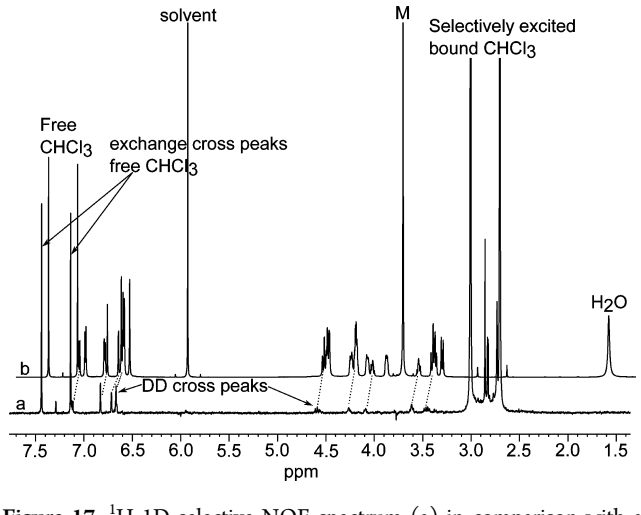

Figure 17. ^{1}H 1D selective NOE spectrum (a) in comparison with a simple ^{1}H spectrum (b) of 10 mM cryptophane-D solution with 46 mM ^{13}C labeled $CHCl_3$ with 1,1,2,2-tetracholroethane-d_2 as solvent at 280 K at 700 MHz with a mixing time of 0.45 s.

considering the eee and EEE columns of Table 7 as the most trustworthy, the distribution of the populated conformations is shown in Figure 18. We can see a significant contribution from the conformers $G_{+2}T_2T_2$, $G_{-2}T_2T_2$, $T_2T_2T_2$, and $G_{-2}G_{-2}G_{-2}$. In particular, it is worthwhile to notice that the $T_2T_2T_2$ conformation, possessing the largest cavity, is highly populated in the presence of the relatively large guest. On the other hand, the very large population of the $G_{-2}G_{-2}G_{-2}$ conformer at the EEE level is surprising. The empirical van der Waals correction is probably exaggerated in this case. The change in the distribution of conformers is also reflected in the chemical shift difference of ^{13}C nuclei of the linkers. The calculated conformationally averaged chemical shift difference ($\delta_{2'}-\delta_{1'}$) in the complex is 4.5 ppm at the low basis set and 4.7 ppm at the high basis set based on the columns eee and EEE that conforms very well with the measured value of 5.5 ppm. Using columns ee and EE the calculated Boltzmann-distribution averaged chemical shift differences are 5.6 and 5.1 ppm, respectively.

The calculations also revealed, in agreement with the ^{1}H NOE measurements, that the geometries with both orientations of chloroform were populated, disregarding which of the methods is judged to be most appropriate. It is important to note that the energy difference between the two orientation of chloroform is the lowest in the case of $T_2T_2T_2$ and without the van der Waals correction (see the Supporting Information).

An interesting behavior of the chemical shift of methoxy groups is found in both the ^{1}H and ^{13}C spectra. A significant exchange broadening and a big chemical shift difference occurs between the complexed and "free" forms. The CH_3 part of the group rotates very fast around the O−C bond, but the dihedral angle 6″−1″−O−M behaves more like other conformational exchange processes. According to the DFT calculations, this angle can attain either a value close to 0 or to 110° and the energy minimization procedure seems to have difficulties finding the deepest minimum. In all four groups of conformers (*GGG*,*GGT*,*GTT*,*TTT*), there was one or two structures which have been optimized with 6″−1″−O−M dihedral angle corresponding to either 0 or 110° minima. The energy change is approximately the same for all the conformers in the same group. So, it is possible to estimate the "optimized" energy for the "missing" conformation. It has been found that the dihedral angle of zero is always lower in energy than that of 110°. The calculated chemical shifts of the two values of the angle (55.9 ppm for the zero dihedral angle and 62.6 ppm for the 110° angle) differ by 6.7 ppm. The calculated absolute value of the chemical shift has a big error, but the difference is in the right range. The methoxy group is in an asymmetric chemical exchange between these two sites. Upon complexation, the population of the sites changes causing a highly shifted position of the average peak. In the spectra, we see that the methoxy groups get more shielded (chemical shift decreases) upon complex formation. This means that it gets closer to the lower chemical shift value, which belongs to the zero dihedral angle according to the calculations. In the case of complexed host, the methoxy group tends to be in the plane of phenyl groups. This is also supported by the crystal structure of cryptophane-D complexed with dichloromethane.[52] The energy difference per methoxy group is the highest in the case of *TTT* (7.2 kJ/mol, B3LYP-6-31G(d)), the zero degree dihedral angle being more stable. The position of the methoxy group is also important in the kinetics of the complexation. As it can be seen in Scheme 1, the methoxy groups constitute a hindrance for the $CHCl_3$ exchange, if the above-mentioned dihedral angle is close to zero. It is thus easier for chloroform to enter or leave the cavity if the dihedral angle is around 110 degree.

dx.doi.org/10.1021/jp303469x | J. Phys. Chem. B 2012, 116, 7898−7913

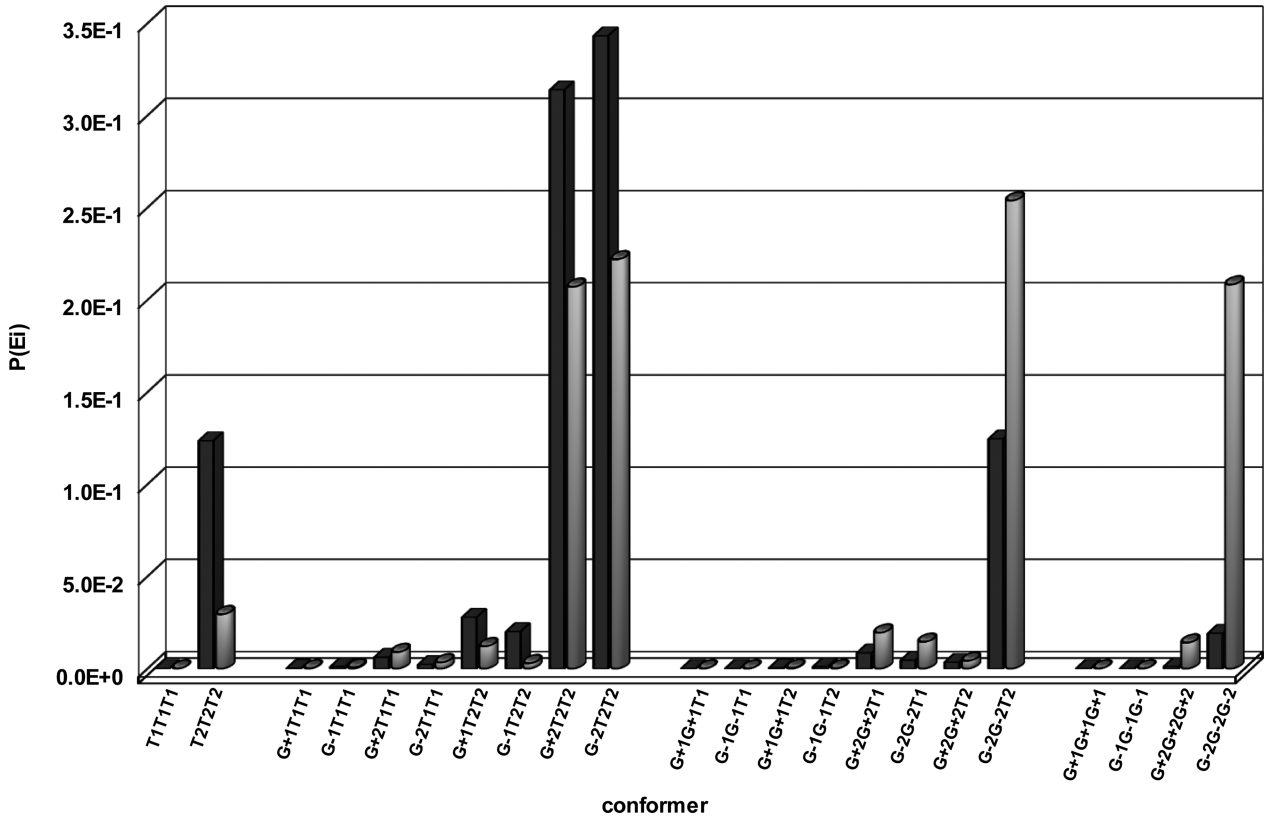

Figure 18. Boltzmann distribution of the calculated conformers for cryptophane-D with chloroform inside the cavity. The black box denotes the basis set 6-31G(d) (optimization) and the gray cylinder the 6-311G+(2d,p) (single-point).

Table 8. Relaxation Rates, NOE Factors, and Motional Parameters of Chloroform at 280 K[a]

	field					
	9.4 T		14.1 T		16.5 T	
^{13}C	R1	NOE	R1	NOE	R1	NOE
free $CHCl_3$	0.092 (0.002)	3.06 (0.42)	0.094 (0.001)	2.90 (0.4)	0.088 (0.002)	2.80 (0.38)
bound $CHCl_3$	3.64 (0.02)	1.58 (0.22)	2.80 (0.02)	1.53 (0.21)	2.37 (0.11)	1.46 (0.20)
S^2 bound $CHCl_3$	0.6 (0.04)					
τ_{loc} (ps) bound $CHCl_3$	34 (9)					

[a]The relaxation rates are given in s^{-1}. The error given in brackets is standard deviation estimated by the Monte Carlo method.

Dynamics of the Guest. We carried out measurements of longitudinal relaxation rates and of the nuclear Overhauser enhancement of chloroform ^{13}C nucleus in several magnetic fields (using the sample containing 10 mM cryptophane-D and 46 mM ^{13}C enriched chloroform). The measurements take long time, even with the ^{13}C enriched chloroform, because of the long relaxation time of the free guest. The longitudinal relaxation of ^{13}C nucleus of both free and bound chloroform species is double exponential due to chemical exchange occurring in a similar time-scale as relaxation. Equations 12−14 were utilized to obtain the true longitudinal relaxation rates and the NOE values for the free and bound guest species (Table 8). The motion of the guest encapsulated in the cryptophane-D host cavity was treated in the framework of the Lipari−Szabo model (eqs 15−17) and described by the parameters of the local motion, the generalized order parameter S^2 = 0.6 and the correlation time of τ_{loc} = 34 ps. The global correlation time of the tumbling of the whole complex was assumed unchanged with respect to the "free" host and the fixed value of 830 ps was used for the calculation. The value of the order parameter of the guest motion is close to the order parameter of the local motion of the linkers in "free" cryptophane-D (vide supra). Thus, the amplitude of reorientation of encapsulated chloroform C−H bond vector on the pico to nanosecond time-scale is strongly restricted down to the level of intrinsic flexibility of the dioxoethylene linkers. The restricted mobility of the chloroform guest inside the cavity is in agreement with the high guest packing coefficient in the crystal structure of a related cryptophane-A derivative.[3] The order parameter also corresponds to a diffusion-in-a-cone motional model[22,53−55] with a semiangle of 32°. Similar behavior was found previously also for the cryptophane-E - chloroform complexes in solution[10] and in the solid state[11] (cryptophane-E contains longer dioxopropylene linkers).

DISCUSSION

On the basis of the above presented results, we can draw an overall picture of the formation of inclusion complexes of cryptophane-D. The free cryptophane-D experiences a

dx.doi.org/10.1021/jp303469x | J. Phys. Chem. B 2012, 116, 7898−7913

substantial conformational flexibility in the region of linkers between its two caps. The DFT calculations showed that several conformations were populated at temperatures close to ambient. The fact that we have never succeeded to remove quantitatively all the guest molecules in the sample preparation procedure gives evidence that the free state of cryptophane-D is strongly disfavored ("horror vacui"). Dichloromethane is an attractive guest with a moderate binding constant that displays very little temperature dependence. The encapsulation of dichloromethane into the host cavity is accompanied by the adaptation of the cavity through conformations of the linkers between caps. This is demonstrated by the changes of chemical shift difference of ^{13}C nuclei 1′ and 2′ with respect to the concentration of dichloromethane (see "inner" lines in Figure 10). The difference, however, never reaches the span of chemical shifts corresponding to encapsulation of the bigger chloroform guest. Chloroform is a less favored guest for cryptophane-D and a large molar excess is needed to achieve a reasonable concentration of the complex. Encapsulation of chloroform leads to decrease of motional freedom of the cryptophane-D linkers in the millisecond (chemical exchange) time-scale. The temperature dependent ^{13}C NMR spectra display significant broadening of the signals belonging to the linkers in the "free" host (i.e., the host that, probably, to a large extent contains encapsulated residual dichloromethane). We interpret the broadening as indicative of fast chemical exchange between several conformations of the linkers thus occurring, roughly, at millisecond time scale. At decreased temperature the transitions become slower, which leads to broadening of the corresponding peaks. Conversely, the peaks corresponding to the cryptophane-D−chloroform complex remain narrow. Furthermore, we determined the mobility of the linkers in the picosecond to nanosecond time scale by means of NMR relaxation measurements. The generalized order parameter $S^2 = 0.55$ of the Lipari−Szabo approach can be converted into a parameter of a specific physical model of the local motion. A realistic one that is commonly used is the diffusion in a cone model. The corresponding cone semi-angle is evaluated as 32°. This value is much smaller than the angular change of the CH bond related to the transition to a different rotameric state which is roughly 60°. Thus, it appears that the picosecond dynamics is related to a random geometry fluctuation within a single rotameric state while transitions between the rotameric states occur at much slower, roughly millisecond time scale.

The barriers (activation energies) for chloroform breaking in and out from the cavity are 47 and 63 kJ mol^{-1}, respectively, similar to the values for dichloromethane. The complex formation free energy yield and its decomposition into enthalpy and entropy reveal a striking difference between the molecular recognition of dichloromethane and chloroform guest that was not noticed earlier. The complexation of dichloromethane is characterized by a favorable change of entropy, while the complexation enthalpy is close to zero. This result suggests no or very limited van der Waals interaction between dichloromethane and the cryptophane-D host. Conversely, the inclusion complex between chloroform and cryptophane-D displays a large favorable enthalpic yield (−17 kJ mol^{-1}) that is evidence of significant attractive dispersion interaction and an entropic penalty of −38 J mol^{-1} K^{-1} that conforms well with the very restricted mobility of chloroform inside of the cavity.

One can speculate that it is also molecular symmetry that plays an important role in the molecular recognition. Symmetry of cryptophane-D is close to the one with 3-fold symmetry axis that is also characteristics of chloroform. Here, we can disregard instantaneous geometries of the very mobile parts of cryptophane: the linkers and the methoxy groups. Thus, the chloroform complex is able to overbalance the loss of entropy and the unfavorable shift in population distribution of conformations of linkers toward elongated geometries, affording largest cavities, perhaps by the attractive C−H···π interaction[57] between hydrogen of chloroform and phenyl rings of cryptophane caps. The distance between the chloroform proton and centers of phenyl rings is 3.3 Å when averaged over calculated structures of all low energy conformers. By contrast, the symmetry incompatibility between cryptophane-D and dichloromethane guest (C_{2v} point group) does not facilitate strong enough attractive dispersion interaction. The entropic yield of almost unrestricted rotational motion[58] of dichloromethane prevails enthalpy of the possible van der Waals interactions. Preference of the most extended cavity geometries when chloroform is encapsuled into cryptophane-A was recently termed as "induced fit"[3] in analogy with the description of protein−ligand interaction proposed by Koshland in the field of structural biology.[59] Our work brings strong evidence that the internal molecular dynamics of cryptophane cavity is inherently involved in the process of guest binding. This feature is characteristic of the so-called conformational selection mechanism. The principle of this mechanism is that the initially broad accessible conformational space of a free host (cf. Figure 2) is significantly narrowed upon binding a guest (ligand). This is a different situation than that assumed by the induced fit, which generally leads to the change of host's original conformation in order to minimize energy of the complex and resulting in a different, previously inaccessible part of the conformational space becoming populated. A significant evidence of importance of conformational selection in the protein−ligand or protein−protein interactions was reported only recently.[56,60−64] We generally cannot exclude the presence of the cryptophane-D with chloroform encapsulated in a conformation that was not populated in the free form, but the observed significant internal mobility of the cryptophane-D linkers at two distinct time scales is more in accordance with the conformational selection picture. It should be added that the subtle interplay between induced fit and conformational selection was recently discussed in the context of protein-peptide interactions.[65]

CONCLUSIONS

Complexes of cryptophane-D with chloroform and dichloromethane were studied using a variety of NMR techniques. The intriguing feature of the results, not discussed extensively in the past, is the sensitivity of the host signals chemical shifts to the presence of guest molecules. In particular, the behavior of the carbon-13 shifts for the linkers connecting the two cyclotribenzylene units is very informative. Our interpretation of these findings, supported by DFT calculations, is that introducing the guests into the cavity results in a conformational selection, i.e., in a major redistribution of possible conformations of the linkers. In particular for the chloroform guest, we observe a significant increase of the $T_2T_2T_2$ conformation. The two guests display chemical exchange between the free and bound sites. The exchange process for chloroform as guest is slow on the NMR time scale, whereas it is fast for dichloromethane over a significant temperature range. Also the thermodynamics of the two complexation reactions is different, with the enthalpy change close to zero for

dichloromethane guest. When both guests are present in solution, they compete for the space in the cavity, so obtaining an empty host cavity does not seem to be possible under mild conditions. For the case of chloroform, we have also investigated the possibility of preferential orientation of the guest inside the cavity through cross-relaxation measurements. Both orientations of the guest, with the C−H bond pointing toward each of the two caps, seem to be equally probable for cryptophane-D, as opposed the case of a similar host, cryptophane-C. For the cryptophane-D−chloroform system, we were also able to measure carbon-13 relaxation for the guest and the host. The data show that the mobility of the chloroform molecule inside the cavity is rather limited.

■ ASSOCIATED CONTENT

Supporting Information

Energies of all optimized structures with a list of dihedral angles and calculated chemical shifts of the linker carbons and methoxy groups, together with the Boltzmann distributions at both basis sets used as well as variable concentration ^{1}H and ^{13}C spectra of 10 mM cryptophane-D−$CHCl_3$ solution. This material is available free of charge via the Internet at http://pubs.acs.org.

■ AUTHOR INFORMATION

Corresponding Author

*E-mail: zoltan.takacs@mmk.su.se; jozef.kowalewski@mmk.su.se.

Notes

The authors declare no competing financial interest.

■ ACKNOWLEDGMENTS

This work was supported by the Swedish Research Council (Grant No. 613-2011-3311). The generous grant from Knut and Alice Wallenberg Foundation, allowing the purchase of the 700 MHz NMR spectrometer for the Arrhenius Laboratory, is gratefully acknowledged. We would like to thank Mr. Torbjörn Astlind for his help with NMR spectrometers and Prof. Margareta Blomberg and Václav Římal for valuable discussions. We also thank Dr. Sven de Marothy for providing the program used to calculate the dispersion corrections.

■ REFERENCES

(1) Brotin, T.; Dutasta, J. P. *Chem. Rev.* **2009**, *109*, 88−130.
(2) Brotin, T.; Roy, V.; Dutasta, J. P. *J. Org. Chem.* **2005**, *70*, 6187−6195.
(3) Taratula, O.; Hill, P. A.; Khan, N. S.; Carroll, P. J.; Dmochowski, I. J. *Nat. Commun.* **2010**, *1*, 148.
(4) Bartik, K.; Luhmer, M.; Dutasta, J. P.; Collet, A.; Reisse, J. *J. Am. Chem. Soc.* **1998**, *120*, 784−791.
(5) Bouchet, A.; Brotin, T.; Cavagnat, D.; Buffeteau, T. *Chem.—Eur. J.* **2010**, *16*, 4507−4518.
(6) Brotin, T.; Cavagnat, D.; Buffeteau, T. *J. Phys. Chem. A* **2008**, *112*, 8464−8470.
(7) Brotin, T.; Cavagnat, D.; Dutasta, J. P.; Buffeteau, T. *J. Am. Chem. Soc.* **2006**, *128*, 5533−5540.
(8) Bouchet, A.; Brotin, T.; Linares, M.; Ågren, H.; Cavagnat, D.; Buffeteau, T. *J. Org. Chem.* **2011**, *76*, 1372−1383.
(9) Takacs, Z.; Soltesova, M.; Kotsyubynskyy, D.; Kowalewski, J.; Lang, J.; Brotin, T.; Dutasta, J. P. *Magn. Reson. Chem.* **2010**, *48*, 623−629.
(10) Lang, J.; Dechter, J. J.; Effemey, M.; Kowalewski, J. *J. Am. Chem. Soc.* **2001**, *123*, 7852−7858.
(11) Nikkhou Aski, S.; Lo, A. Y. H.; Brotin, T.; Dutasta, J. P.; Edén, M.; Kowalewski, J. *J. Phys. Chem. C* **2008**, *112*, 13873−13881.
(12) Tosner, Z.; Lang, J.; Sandström, D.; Petrov, O.; Kowalewski, J. *J. Phys. Chem. A* **2002**, *106*, 8870−8875.
(13) Binsch, G. In *Topics in steroechemistry*; Allinger, N. L., Eliel, E. L., Eds.; John Wiley Sons, Inc.: Hoboken, NJ, 1968; Vol. 3, pp 97−191.
(14) Římal, V.; Štěpánková, H.; Štěpánek, J. *Concepts Magn. Reson.* **2011**, *38A*, 117−127.
(15) McConnell, H. M. *J. Chem. Phys.* **1958**, *28*, 430−431.
(16) Bain, A. D.; Duns, G. J. *Can. J. Chem.* **1996**, *74*, 819−824.
(17) Kowalewski, J.; Mäler, L. *Nuclear Spin Relaxation in Liquids:Theory,Experiments, and Applications*; Taylor & Francis: London, 2006.
(18) Gutowsky, H. S.; Holm, C. H. *J. Chem. Phys.* **1956**, *25*, 1228−1234.
(19) Kaplan, J. *J. Chem. Phys.* **1958**, *28*, 278−282.
(20) Bain, A. D. *Progr. NMR Spectr.* **2003**, *43*, 63−103.
(21) Bloch, F. *Phys. Rev.* **1946**, *70*, 460−474.
(22) Lipari, G.; Szabo, A. *J. Am. Chem. Soc.* **1982**, *104*, 4546−4559.
(23) Solomon, I. *Phys. Rev.* **1955**, *99*, 559−565.
(24) Canceill, J.; Lacombe, L.; Collet, A. *C. R. Acad. Sci. Ser. II* **1984**, *298*, 39−42.
(25) Wokaun, A.; Ernst, R. R. *Chem. Phys. Lett.* **1977**, *52*, 407−412.
(26) Palmer, A. G., III; Cavanagh, J.; Wright, P. E.; Rance, M. *J. Magn. Reson.* **1991**, *93*, 151−170.
(27) Willker, W.; Leibfritz, D.; Kerssebaum, R.; Bermel, W. *Magn. Reson. Chem.* **1993**, *31*, 287−292.
(28) Zwahlen, C.; Legault, P.; Vincent, S. J. F.; Greenblatt, J.; Konrat, R.; Kay, L. E. *J. Am. Chem. Soc.* **1997**, *119*, 6711−6721.
(29) Boyer, R. D.; Johnson, R.; Krishnamurthy, K. *J. Magn. Reson.* **2003**, *165*, 253−259.
(30) Kay, L. E.; Keifer, P.; Saarinen, T. *J. Am. Chem. Soc.* **1992**, *114*, 10663−10665.
(31) Schleucher, J.; Schwendinger, M.; Sattler, M.; Schmidt, P.; Schedletzky, O.; Glaser, S. J.; Sorensen, O. W.; Griesinger, C. *J. Biomol. NMR* **1994**, *4*, 301−306.
(32) Cicero, D. O.; Barbato, G.; Bazzo, R. *J. Magn. Reson.* **2001**, *148*, 209−213.
(33) Stott, K.; Keeler, J.; Van, Q. N.; Shaka, A. J. *J. Magn. Reson.* **1997**, *125*, 302−324.
(34) Emsley, L.; Bodenhausen, G. *Chem. Phys. Lett.* **1990**, *165*, 469−476.
(35) Macura, S.; Farmer, B. T.; Brown, L. R. *J. Magn. Reson.* **1986**, *70*, 493−499.
(36) Hu, H. T.; Krishnamurthy, K. *J. Magn. Reson.* **2006**, *182*, 173−177.
(37) Zhou, Z.; Kümmerle, R.; Qiu, X. H.; Redwine, D.; Cong, R. J.; Taha, A.; Baugh, D.; Winniford, B. *J. Magn. Reson.* **2007**, *187*, 225−233.
(38) Kowalewski, J.; Ericsson, A.; Vestin, R. *J. Magn. Reson.* **1978**, *31*, 165−169.
(39) Frisch, M. J.; et al. *Gaussian 09*, revision A.02; Gaussian, Inc.: Wallingford, CT, 2009.
(40) de Dios, A. C. *Progr. NMR Spect.* **1996**, *29*, 229−278.
(41) Barone, V.; Cossi, M. *J. Phys. Chem. A* **1998**, *102*, 1995−2001.
(42) Cossi, M.; Rega, N.; Scalmani, G.; Barone, V. *J. Comput. Chem.* **2003**, *24*, 669−681.
(43) Grimme, S. *J. Comput. Chem.* **2006**, *27*, 1787−1799.
(44) Riley, K. E.; Pitonak, M.; Jurecka, P.; Hobza, P. *Chem. Rev.* **2010**, *110*, 5023−5063.
(45) Jones, T. A.; Zou, J. Y.; Cowan, S. W.; Kjeldgaard, M. *Acta Crystallogr.* **1991**, *A47*, 110−119.
(46) Kleywegt, G. J.; Jones, T. A. *Acta Crystallogr.* **1994**, *D50*, 178−185.
(47) Kleywegt, G. J.; Jones, T. A. *Biomacromolecular Speleology. CCP4/ESF-EACBM Newsletter on Protein Crystallography* **1993**, *29*, 26−28.
(48) Kleywegt, G. J.; Zou, J. Y.; Kjeldgaard, M.; Jones, T. A. *International Tables for Crystallography, Vol. F. Crystallography of*

Biological Macromolecules; Rossmann, M. G., Arnold, E., Eds.; Wiley: Dordrecht, 2001; pp 353−356, 366−367.
(49) Cuc, D.; Bouguet-Bonnet, S.; Morel-Desrosiers, N.; Morel, J. P.; Mutzenhardt, P.; Canet, D. *J. Phys. Chem. B* **2009**, *113*, 10800−10807.
(50) Nikkhou Aski, S.; Takacs, Z.; Kowalewski, J. *Magn. Reson. Chem.* **2008**, *46*, 1135−1140.
(51) Liu, L.; Guo, Q. X. *J. Inc. Phenom. Macrocycl. Chem.* **2002**, *42*, 1−14.
(52) Canceill, J.; Cesario, M.; Collet, A.; Guilhem, J.; Pascard, C. *J. Chem. Soc. Chem. Commun.* **1985**, 361−363.
(53) Lipari, G.; Szabo, A. *J. Am. Chem. Soc.* **1982**, *104*, 4559−4570.
(54) Daragan, V. A.; Mayo, K. H. *Progr. NMR Spectr.* **1997**, *31*, 63−105.
(55) Jarymowycz, V. A.; Stone, J. M. *Chem. Rev.* **2006**, *106*, 1624−1671.
(56) Tsai, C. J.; Kumar, S.; Ma, B. Y.; Nussinov, R. *Protein Sci.* **1999**, *8*, 1181−1190.
(57) Takahashi, H.; Tsuboyama, S.; Umezawa, Y.; Honda, K.; Nishio, M. *Tetrahedron* **2000**, *56*, 6185−6191.
(58) Akke, M.; Brüschweiler, R.; Palmer, A. G. *J. Am. Chem. Soc.* **1993**, *115*, 9832−9833.
(59) Koshland, D. E. *Proc. Natl Acad. Sci. U.S.A.* **1958**, *44*, 98−104.
(60) Goh, C. S.; Milburn, D.; Gerstein, M. *Curr. Opin. Struct. Biol.* **2004**, *14*, 104−109.
(61) Lange, O. F.; Lakomek, N. A.; Fares, C.; Schröder, G. F.; Walter, K. F. A.; Becker, S.; Meiler, J.; Grubmüller, H.; Griesinger, C.; de Groot, B. L. *Science* **2008**, *320*, 1471−1475.
(62) Wlodarski, T.; Zagrovic, B. *Proc. Natl. Acad. Sci. U.S.A.* **2009**, *106*, 19346−19351.
(63) Miller, Y.; Ma, B. Y.; Nussinov, R. *Proc. Natl. Acad. Sci. U.S.A.* **2010**, *107*, 9490−9495.
(64) Srb, P.; Vlach, J.; Prchal, J.; Grocky, M.; Ruml, T.; Lang, J.; Hrabal, R. *J. Phys. Chem. B* **2011**, *115*, 2634−2644.
(65) Anthis, N. J.; Doucleff, M.; Clore, M. G. *J. Am. Chem. Soc.* **2011**, *133*, 18966−18974.